# Random Ginzburg-Landau model revisited: Reentrant phase transitions

Javier Buceta,[1] Juan M. R. Parrondo,[2] and F. Javier de la Rubia[1]
[1]*Departamento de Física Fundamental, Universidad Nacional de Educación a Distancia, Apartado de Correos 60.141, 28040 Madrid, Spain*
[2]*Departamento de Física Atómica, Molecular y Nuclear, Facultad de Ciencias Físicas, Universidad Complutense de Madrid, Ciudad Universitaria s/n, 28040 Madrid, Spain*
(Received 20 June 2000; published 20 February 2001)

We analyze the phase diagram of the random Ginzburg-Landau model, where a quenched dichotomous noise affects the control parameter. We show that the system exhibits two types of counterintuitive reentrant second-order phase transitions. In the first case, increasing the coupling drives the system from a disordered to an ordered state and then back to a disordered state. In the second case, increasing the intensity of the quenched noise, the system goes from an ordered phase to a disordered phase and back to an ordered state. We discuss the general mechanism that produces these reentrant phase transitions, showing that it may appear in other physical systems, such as a modification of the spin-1 Blume-Capel model proposed to describe the critical behavior of helium mixtures in a random medium.

DOI: 10.1103/PhysRevE.63.031103 PACS number(s): 05.40.−a, 68.35.Rh, 64.60.Cn

## I. INTRODUCTION

Random impurities play a crucial role in the physical properties of many systems. For example, in a ferromagnetic material the inclusion of random impurities shifts the critical temperature, modifies the critical exponents, and can even suppress the ferromagnetic phase when the proportion of impurities exceeds a certain threshold [1]. Parallel to experimental studies with technological motivations, a lot of effort has been made from the early seventies to theoretically characterize the critical behavior and phase diagrams of these systems [2,3].

Restricting ourselves to theoretical studies, we will briefly review the effect of disorder and external fluctuations on the paradigmatic model of equilibrium phase transitions: the time-dependent Ginzburg-Landau (GL) model, also referred to as model *A*, on a lattice [4,5].

Model *A* can be derived from the Ising model by means of a coarse-graining procedure [6]. It describes the critical behavior of anisotropic ferromagnet systems [4], and the dynamics of front propagation [7]. Moreover, the GL Hamiltonian describes the critical behavior of many physical systems as it can be interpreted as an expansion of the free energy around the critical point [5].

Random impurities can be included in the GL model as external fluctuations perturbing the coefficients of the Hamiltonian. This procedure can be justified by both microscopic and phenomenological arguments [6], and it has been used to study the influence of inhomogeneities in superconductors [8,9]. However, near the critical point, a perturbative expansion shows that only the fluctuations of the control parameter are relevant [6].

Usually, the fluctuations are considered Gaussian distributed, and the model is known as random GL model or $\phi^4$ model with random temperature. This model has been investigated using renormalization group methods, concluding that randomness in the control parameter causes the appearance of a new random fixed point [6]. More recent studies [10] have revealed that replica symmetry is broken in the paramagnetic phase far away from the critical point, suggesting that a deeper investigation of the physics of phase transitions in random ferromagnets is necessary. Short and long-range correlated quenched impurities have been also considered for model *A* [11], leading to relevant corrections of the mean-field value of critical exponents. Nevertheless, to our knowledge, there is no complete characterization of the phase diagram and the reentrant phenomena in these random models.

From the point of view of nonequilibrium statistical mechanics, there are relevant studies of the time-dependent GL model perturbed by Gaussian white noise in the control parameter [12,13]. For this case, a mean-field analysis, confirmed by extensive numerical simulations, shows that multiplicative white noise can play a counterintuitive role. For some values of the coupling, noise can induce the appearance of an ordered phase [12]. The system also undergoes reentrant transitions [13], which are the result of a nontrivial interaction between diffusive coupling and multiplicative noise in spatially extended systems.

This unexpected and constructive role of external fluctuations on spatially extended systems has been a subject of increasing interest in recent years [14–18]. As we have just mentioned, noise can induce ordered phases, reentrant first and second order phase transitions, and even ordered spatial structures. More recently [19,20], colored noise has been studied in the pure noise-induced phase transition model introduced in [15], bringing out new effects when the correlation time of the external fluctuations changes. For instance, in addition to the reentrant phase transition as a function of the noise intensity, the model presents a new reentrant transition when the coupling is increased [19] as well as metastability regions [20]. However, the effect of colored noise on the GL equation has been limited only to the additive case [21].

In this paper we study the phase diagram of the time-dependent GL model, model *A*, with quenched dichotomous impurities, i.e., with a dichotomous multiplicative noise of infinite correlation-time perturbing the control parameter. This is an equilibrium problem which, nevertheless, exhibits reentrant transitions akin to those found in the field of non-

 

equilibrium noise-induced phase transitions. Therefore, the present study can be considered as part of the two research lines that we have briefly described in the above paragraphs: equilibrium systems with disorder and nonequilibrium noise-induced phase transitions. We use and benefit from the techniques of both fields.

We will see that the inclusion of such a disorder produces several relevant results. In particular, we show that the model exhibits two types of reentrant second-order phase transitions. The first one drives the system from a disordered state to an ordered state and back to a disordered one by increasing the coupling, as in the pure noise-induced phase transition models with colored noise. The second transition: order-disorder-order by increasing the multiplicative noise intensity, has no precedent, to our knowledge, in the literature. We also study the dependence of the phase diagram on the proportion of impurities.

The structure of the paper is the following. In Sec. II we present the model and the mean-field analysis. In Sec. III we describe and discuss the phase diagram of the model and its reentrant phase transitions. In Sec. IV we present numerical simulations in a two-dimensional lattice that qualitatively confirm the previous theoretical analysis. In Sec. V we give an intuitive explanation of several reentrant transitions using a decimation technique, and show the generality of the mechanism that produces the main features of the model, illustrating the idea with a variant of the Blume-Capel model [22] proposed to model the critical behavior of helium mixtures in a random medium. Finally, in Sec. VI we summarize the main conclusions and present the perspectives of future work in this field.

## II. MODEL: MEAN-FIELD ANALYSIS

Consider a scalar field defined on a $d$-dimensional square lattice $\{\psi_i\}$. The time-dependent GL model with dichotomous quenched impurities is given by the following dimensionless Langevin equation:

$$\partial_t \psi_i = (\alpha + \zeta_i)\psi_i - \psi_i^3 + \frac{D}{2d}\sum_{\langle ji\rangle}(\psi_j - \psi_i) + \eta_i, \qquad (1)$$

where the sum runs over the $2d$ nearest neighbors of site $i$, and $\eta_i$ are Gaussian white noises with zero mean and correlation

$$\langle \eta_i(t)\,\eta_j(t')\rangle = \delta_{ij}\delta(t-t'). \qquad (2)$$

The quenched multiplicative noises $\zeta_i$ mimic the presence of disorder. They are Markovian dichotomous processes spatially uncorrelated and with infinite correlation time. The probability density of the impurities is

$$P(\zeta_i) = p_+\,\delta(\zeta_i - \Delta) + p_-\,\delta(\zeta_i + \Delta), \qquad (3)$$

where $p_\pm$ denotes the probability that the noise takes the $\pm\Delta$ value. Note that, when referring to the impurities, the terms *probability* and *proportion* can be exchanged in the thermodynamic limit, since then $p_\pm$ is equal to the proportion of $\pm\Delta$ impurities.

As we said before, in the context of anisotropic ferromagnets, the control parameter, $\alpha$, measures the distance to the critical temperature. In this way, Eq. (1) could serve as a model for the evolution of the local magnetization in a conglomerate of two anisotropic ferromagnets with different critical temperatures.

The stationary solution of Eq. (1), for a given configuration of the disorder, is the equilibrium Gibbs state

$$\rho = \frac{\exp[-\beta\mathcal{H}(\{\psi_i\};\{\zeta_i\})]}{\mathcal{Z}}, \qquad (4)$$

where, due to Eq. (2) and the fluctuation-dissipation theorem, $\beta = 2$. The Hamiltonian is given by

$$\mathcal{H}(\{\psi_i\};\{\zeta_i\}) = \sum_{i=1}^{N}\left\{V(\psi_i;\zeta_i) + \frac{D}{8d}\sum_{\langle ji\rangle}(\psi_j - \psi_i)^2\right\} \qquad (5)$$

and the local potential at each site is

$$V(\psi_i;\zeta_i) = -\frac{(\alpha+\zeta_i)}{2}\psi_i^2 + \frac{\psi_i^4}{4}. \qquad (6)$$

The sign of the quadratic term of the potential determines the local dynamics at each site. If $(\alpha+\zeta_i)<0$, we have a single well potential with a single equilibrium point at $\psi_i = 0$. On the other hand, if $(\alpha+\zeta_i)>0$, the state $\psi_i = 0$ becomes unstable and $V(\psi_i;\zeta_i)$ is a double well potential with two symmetric stable points at $\psi_i = \pm\sqrt{\alpha+\zeta_i}$.

For an estimation of the phase diagram of the model, we use a Weiss mean-field approximation for spatially extended systems [12]. Replacing, in the diffusive term, the field at the nearest neighbors by the mean value, $\langle\psi\rangle$, we can drop the lattice index and write down the following equation for the temporal evolution of the field at a generic site:

$$\partial_t \psi = (\alpha+\zeta)\psi - \psi^3 + D(\langle\psi\rangle - \psi) + \eta, \qquad (7)$$

where $\zeta$ is a random variable with a probability distribution given by Eq. (3). This equation is equivalent to the system

$$\partial_t \psi_\pm = (\alpha \pm \Delta)\psi_\pm - \psi_\pm^3 + D(\langle\psi\rangle - \psi_\pm) + \eta, \qquad (8)$$

where $\psi_\pm$ is the field at a site where $\zeta = \pm\Delta$.

Equation (7) is not a closed evolution equation for the stochastic process $\psi$, but it can be easily solved in the stationary regime with $\langle\psi\rangle$ as a parameter. The stationary solution reads:

$$P_{\rm st}(\psi;\langle\psi\rangle) = p_+ P_{\rm st}^+(\psi;\langle\psi\rangle) + p_- P_{\rm st}^-(\psi;\langle\psi\rangle), \qquad (9)$$

where $P_{\rm st}^\pm(\psi;\langle\psi\rangle)$ are the stationary probability densities for the two dynamics defined by Eq. (8). These probability densities are

$$P_{\rm st}^\pm(\psi;\langle\psi\rangle) = N^\pm \exp\{-2[V(\psi;\pm\Delta) + D\psi(\psi - \langle\psi\rangle)]\}, \qquad (10)$$

where the potential $V(\psi;\zeta)$ is defined in Eq. (6) and $N^\pm$ are normalization constants.

Finally, the following self-consistent condition must be fulfilled:

$$\langle \psi \rangle = \int_{\mathbb{R}} \psi P_{\rm st}(\psi;\langle \psi \rangle) \mathrm{d}\psi. \tag{11}$$

This equation has $\langle \psi \rangle = 0$ as a solution for any value of the parameters. This solution is called the *disordered phase*. However, nonsymmetric solutions exist in some regions of the space of parameters. These solutions with $\langle \psi \rangle \neq 0$ are called *ordered phases*. A phase transition occurs when the system is driven from a region with only the symmetric solution to a region with ordered phases.

According to the mean-field theory, phase transitions occur at those values of the parameters satisfying the condition [12]

$$\int_{\mathbb{R}} \psi \frac{\partial P_{\rm st}(\psi;\langle \psi \rangle)}{\partial \langle \psi \rangle}|_{\langle \psi \rangle = 0} d\psi = 2D \int_{\mathbb{R}} \psi^2 P_{\rm st}(\psi;0) d\psi = 1. \tag{12}$$

Equations (11) and (12) can be also derived using a replica trick calculation to average the quenched disorder with the replica symmetry ansatz (see the Appendix for details).

In the case $p_+ = 1$ or $p_- = 1$, the phase boundaries are equivalent to the standard model *A*. This phase diagram has been studied with both the mean-field technique [12,23] and $2d$ numerical simulations [5].

### III. PHASE DIAGRAM

Let us first discuss the phase diagram in the plane $(\Delta, D)$ given by Eq. (12). We distinguish two cases: $\alpha < 0$ and $\alpha > 0$.

For $\alpha$ negative and $\Delta < |\alpha|$, it is obvious that no ordered phase can exist, since $\psi = 0$ is stable in the two possible local potentials (6). On the other hand, if $\Delta > |\alpha|$ a fraction $p_+$ of sites feels a double well potential and then, for strong enough coupling $D$, an ordered phase may appear. In Fig. 1 we plot the phase diagram for $\alpha = -0.75$ and several values of $p_+$. Note that, below a certain value of $p_+$, a reentrant transition disorder-order-disorder (DOD) with the coupling appears. That is, by continuously increasing the coupling we can first drive the system from a disordered to an ordered state, as in the standard model *A*, and then back to a disordered state. This reentrant phenomenon is always present in the system below that critical value of $p_+$. Note that by decreasing $p_+$ the ordered phase shifts to the right, due to the fact that the fraction of double-well local potentials decreases and then these potentials have to be deeper, i.e., $\Delta$ must be larger, in order to keep stable the ordered phase. The reentrant transition increasing $D$ is clearly indicated by the behavior of the order parameter, $m = |\langle \psi \rangle|$, as plotted in Fig. 2 where $\Delta = 4$ and $p_+ = 0.3$.

For $\alpha > 0$, the model presents a richer phenomenology than in the previous case. If $\Delta < \alpha$, every site feels a double well potential and therefore an ordered phase appears for a given value of the coupling. On the other hand, if $\Delta > \alpha$ the competition between the two dynamics produces new transitions depending on the value of $p_+$. In Fig. 3 we plot the phase boundaries for $\alpha = 0.75$. There is a topological change around $p_+ = 0.22$: below this value, the region of disordered states is connected and the region of ordered states is disconnected (see for instance the curve for $p_+ = 0.2$, whereas above $p_+ = 0.22$ it is the other way around (see $p_+ = 0.225$). Note that in this case there are two kinds of reentrant phase transitions: the one described previously (DOD) and a new one order-disorder-order (ODO) increasing the noise intensity $\Delta$. This new reentrant phase transition appears above a given value of the coupling. In Fig. 4 we show the ODO transition by plotting the order parameter as a function of $\Delta$ for $D = 4$ and $p_+ = 0.2$.

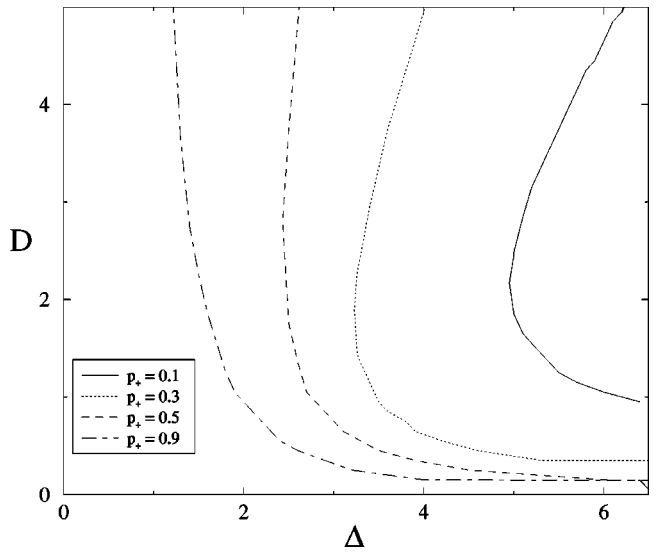


FIG. 1. Phase diagram for $\alpha = -0.75$ and different values of $p_+$. The ordered regions are located to the right of the phase boundaries. The possibility of DOD reentrant phase transitions depends on the value of $p_+$.

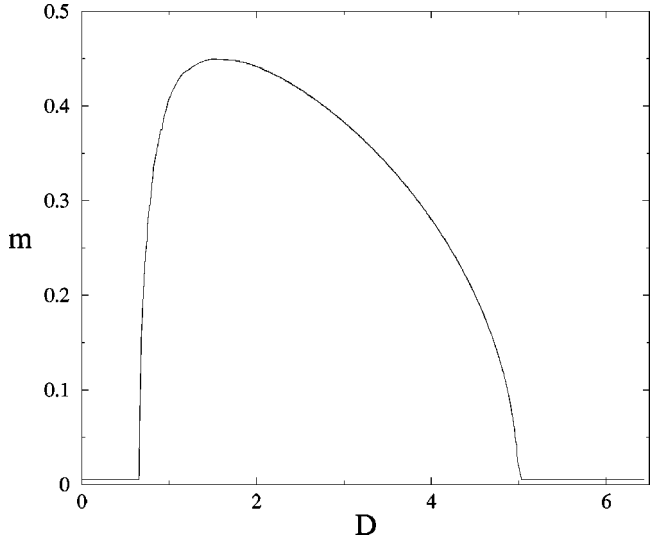


FIG. 2. Order parameter as a function of the coupling $D$ for $p_+ = 0.3$, $\alpha = -0.75$, and $\Delta = 4$.

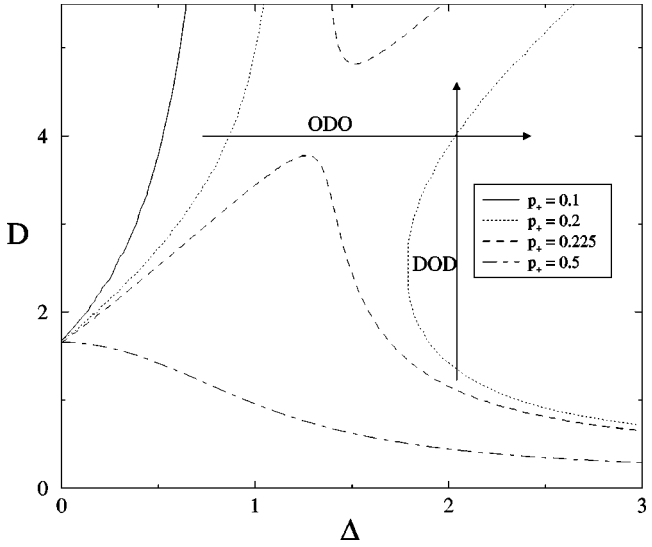


FIG. 3. Phase diagram for $\alpha=0.75$ and different values of $p_+$. Note the saddle point behavior that appears varying $p_+$ and the two kinds of reentrant phase transitions, DOD and ODO, indicated by the arrows.

## IV. NUMERICAL SIMULATIONS

We also performed computer simulations of the model in two dimensions for different system sizes, $L\times L$, varying from $L=10$ to $L=30$. We measured several critical quantities in the simulations [5,15]: the order parameter $m=\langle|L^{-2}\Sigma\psi_i|\rangle$, the susceptibility $\chi=\beta L^2[\langle m^2\rangle-\langle m\rangle^2]$ with $\beta=2$, and the second-order cumulant $\kappa_2=\langle m^2\rangle/\langle m\rangle^2$. Here $\langle\cdot\rangle$ denotes average over time and over disorder realizations once the equilibrium state is reached. We typically average over one thousand configurations of disorder. Finite-size scaling theory predicts that the second-order cumulant does not depend on the size of the system at the critical point [24], providing an accurate method to determine the position of the critical points.

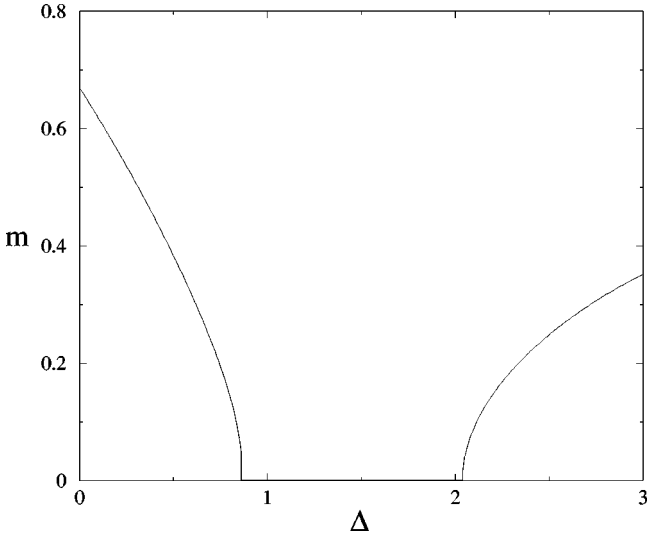


FIG. 4. Order parameter as a function of $\Delta$ ($p_+=0.2$, $\alpha=0.75$, $D=4$). The shape of the curve indicates the ODO reentrant phase transition mentioned in the text.

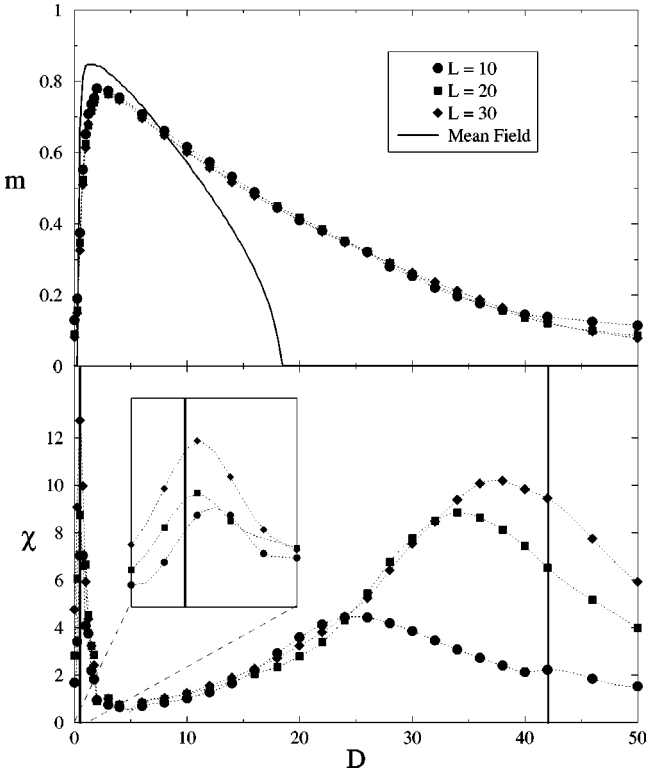


FIG. 5. Simulation results for the order parameter $m$ and the susceptibility $\chi$ as a function of the coupling. The value of the parameters are $\alpha=-0.75$, $\Delta=4$, and $p_+=0.5$. We also plot the mean-field order parameter (solid line) and two vertical wide solid lines indicating the location of the critical points. The inset graph shows details of the susceptibility at small $D$.

In Fig. 5 we plot the numerical simulation results of the order parameter and the susceptibility as a function of the coupling for $\alpha=-0.75$, $\Delta=4$, and $p_+=0.5$. Notice that the reentrant DOD behavior of the order parameter is in qualitative agreement with the mean-field order parameter also plotted in the figure. The behavior of the susceptibility, also plotted in Fig. 5, at the critical points with the two peaks becoming higher as the size of the system increases, proves the presence of two second-order phase transitions. Vertical wide solid lines in Fig. 5 indicate the locations of the entrant and reentrant phase transitions obtained by means of the second-order cumulant technique.

Figure 6 is analogous to the previous one but for $\alpha=0.75$, $D=9$, $p_+=0.2$, and varying $\Delta$. In this case we have an ODO reentrant phase transition by increasing the multiplicative noise intensity. We also notice that the susceptibility behaves at the critical points in a way similar to the previous case indicating again the existence of second-order phase transitions. The second-order cumulant has been used to locate the entrant and reentrant critical points, indicated again by wide solid lines in Fig. 6.

Figures 5 and 6 show a novel and interesting feature of the mean-field approximation. In equilibrium and in most nonequilibrium phase transitions [12,13,15], this approximation overestimates the size of the regions in the phase diagram with ordered phases. This could be expected since, in the mean-field approximation, all the sites interact with each

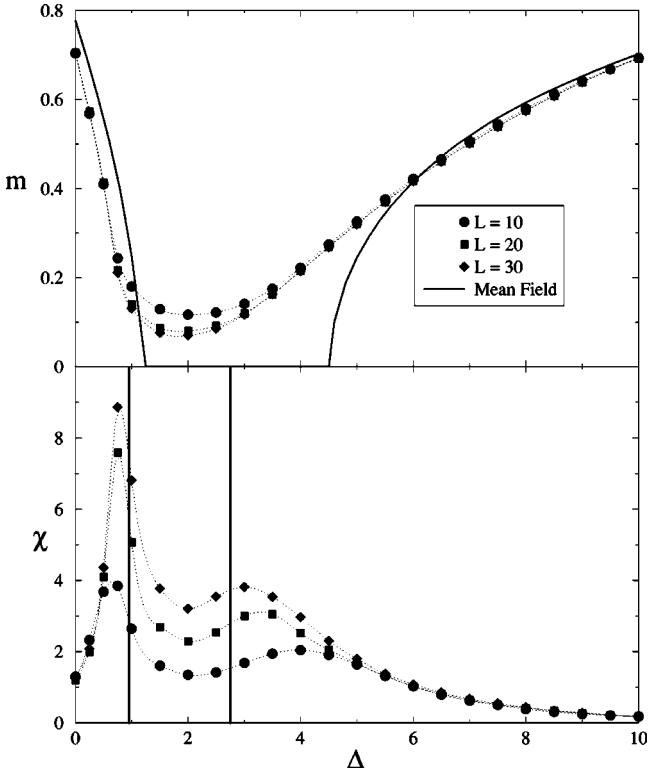


FIG. 6. Order parameter $m$ and susceptibility $\chi$ obtained from numerical simulations varying $\Delta$ ($\alpha=0.75$, $D=9$, and $p_+=0.2$). We also plot the mean-field order parameter (solid line) and the positions of the critical points with two vertical wide solid lines.

other. However, in our case the mean-field approximation underestimates these regions. This fact has also been found in a nonequilibrium model with colored noise [19] and we conjecture that it is related to the existence of an order-disorder transition with the coupling.

## V. DISCUSSION

In this section we explore the mechanisms underlying the phase transitions reported above.

The mechanism for the ODO reentrant transition as a function of $\Delta$ for $\alpha>0$ and $p_+$ small could be described as follows. If $\Delta=0$, all the local potentials have a double well structure and then, if the coupling is strong enough, the system is in an ordered phase. When $\Delta>\alpha$, the local potential of the $p_-$ sites have a single well and as a consequence, an order-disorder transition is induced. If we further increase $\Delta$, the influence of $p_-$ sites fades out inducing the disorder-order phase transition. The reason is that for the double well potentials, the depth of the minima decreases as $-(\alpha+\Delta)^2/4$, whereas the minimum value of the single well potential remains equal to zero for any value of $\Delta$.

We will focus now on the DOD phase transitions as a function of the coupling. These transitions occur for $\alpha+\Delta>0$, $\alpha-\Delta<0$, and $p_+$ small, i.e., when sites with negative multiplicative noise feel a single well potential, and sites with positive noise, which are a small fraction $p_+$ of the system, feel a double well potential. In this case, we can visualize the system as a small number of particles in double well potentials [we will refer to them as double well (DW) sites] surrounded by particles in single well potentials [single well (SW) sites].

When the coupling between sites is zero, there is no ordered phase; particles in SW sites fluctuate around zero, whereas those in DW sites fluctuate either around the negative or the positive minimum of the potential. The total ''magnetization,'' i.e., the average of the field, is therefore zero. If we increase the coupling and the double wells are deep enough, the DW sites act as ''seeds'' of domains with positive or negative magnetization. These domains possess a kind of surface tension due to the coupling, and eventually one of them grows covering the whole system. However, if the coupling is strong enough, the SW sites surrounding the DW sites do not allow the creation of such domains.

This intuitive argument explains how the reentrant transition with the coupling occurs. However, it can be translated into a more quantitative theory that we call *decimation technique*.

### A. Decimation

A decimation theory can be introduced for a globally coupled random GL model. The idea is to integrate out the SW sites, i.e., those sites where $\alpha-\Delta$ takes a negative value, in the partition function:

$$\mathcal{Z}=\int_{\mathbb{R}^N} d\vec{\psi}\,\exp[-\beta\mathcal{H}_{GC}(\{\psi_i\};\{\zeta_i\})], \tag{13}$$

where $d\vec{\psi}=\Pi_{i=1}^{N} d\psi_i$ and the Hamiltonian is given by

$$\mathcal{H}_{GC}(\{\psi_i\};\{\zeta_i\})=\sum_{i=1}^{N}\left\{V(\psi_i;\zeta_i)+\frac{D}{4N}\sum_{j=1}^{N}(\psi_j-\psi_i)^2\right\}. \tag{14}$$

In order to obtain simple analytic expressions, we approximate the local potential at SW sites by a parabolic potential, i.e.,

$$V(\psi_i;-\Delta)=-\frac{\alpha-\Delta}{2}\psi_i^2+\frac{1}{4}\psi_i^4\simeq-\frac{\alpha-\Delta}{2}\psi_i^2. \tag{15}$$

The approximation is valid if $\alpha-\Delta<0$ and the field is small enough. The decimation process, carried out on a globally coupled random GL model, yields the approximate partition function:

$$\mathcal{Z}\propto\int_{\mathbb{R}^{N_+}} d\vec{\psi}_+\exp(-\beta\tilde{\mathcal{H}}_{GC}[\{\psi_i\}_{i\in S^+}]), \tag{16}$$

where $d\vec{\psi}_+\equiv\Pi_{i\in S^+}d\psi_i$ and $S^+$ is the set of DW sites, i.e., the set of sites where the noise is $\zeta_i=\Delta$. The number of these sites is approximately $N_+\equiv Np_+$. The effective Hamiltonian is:

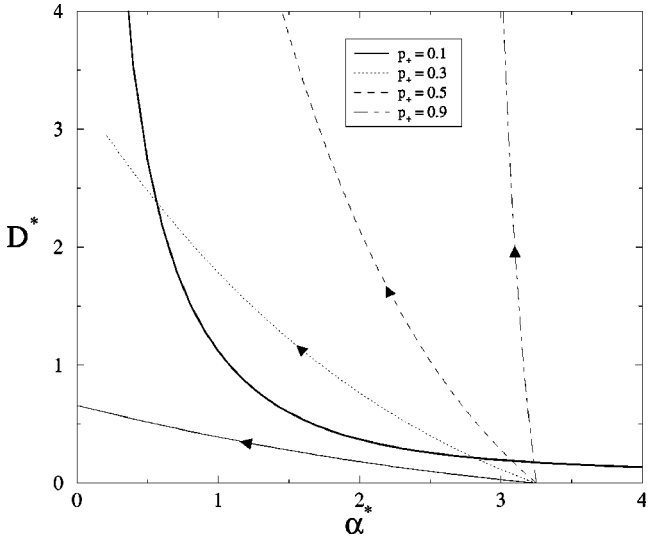


FIG. 7. Decimation technique trajectories for different values of $p_+$ ($\alpha=-0.75$, $\Delta=4$). The wide solid line indicates the mean-field phase diagram of the nonrandom model *A*. The arrows indicate the direction of the trajectories as one increases *D*.

$$\tilde{\mathcal{H}}_{GC}(\{\psi_i\}_{i\in S^+})=\sum_{i\in S^+}\left\{-\frac{\alpha^*}{2}\psi_i^2+\frac{1}{4}\psi_i^4+\frac{D^*}{4N_+}\sum_{j\in S^+}(\psi_j-\psi_i)^2\right\}. \tag{17}$$

This Hamiltonian has the same functional form as the Hamiltonian of a *nonrandom* GL model with $N_+$ sites [cf. Eqs. (17) and (14) and (15) with $\Delta=0$). The parameters of the effective Hamiltonian are given by

$$\alpha^*=\alpha+\Delta+\frac{D(1-p_+)(\alpha-\Delta)}{Dp_++\Delta-\alpha},$$
$$D^*=Dp_+\frac{D+\Delta-\alpha}{Dp_++\Delta-\alpha}. \tag{18}$$

Therefore, the DW sites of the original model now form a nonrandom GL system with effective coupling $D^*$ and effective control parameter $\alpha^*$. Figure 7 depicts the mean-field phase diagram of a nonrandom GL model in the plane $(D^*,\alpha^*)$. For given values of $D$, $\alpha$, $p_+$, and $\Delta$ in the original model, by applying the transformation given by Eq. (18), one can check whether $(D^*,\alpha^*)$ is in the region of ordered or disordered phase. In the same way, we can map trajectories in the original space of parameters $(D,\alpha,\Delta,p_+)$ into trajectories in the phase diagram of Fig. 7.

For $\Delta$, $\alpha$, and $p_+$ constant, $D^*$ is an increasing function of $D$, whereas $\alpha^*$ is decreasing. This can be easily explained: the coupling $D^*$ between DW sites in the decimated system increases with the coupling $D$ in the original model; on the other hand, the effective control parameter $\alpha^*$ decreases due to the influence of the decimated SW sites. It can even be negative, i.e., those sites that were DW sites in the original model become SW sites after the decimation.

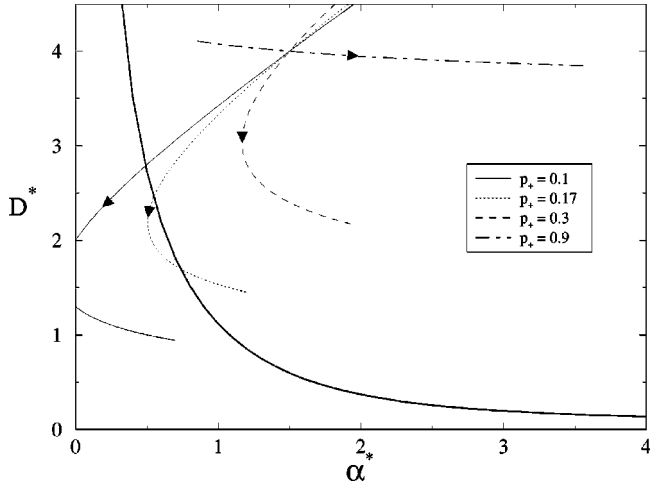


FIG. 8. Increasing $\Delta$ trajectories calculated by the decimation method for $\alpha=0.75$, $D=4$, and different values of $p_+$. The wide solid line represents the mean-field phase boundaries of the nonrandom model *A* and the arrows the direction of the trajectories as one increases $\Delta$.

The four trajectories in Fig. 7 start at $D^*=0$ and $\alpha^*=\alpha+\Delta=3.25$ ($D=0$). This point is obviously in the disordered phase region. The trajectories then move upwards and some of them enter into the ordered phase region. This first disorder-order transition is due to the increase of the effective coupling $D^*$. For some values of $p_+$ ($p_+=0.3$ in Fig. 7), the trajectories get back to the disordered phase region through a reentrant phase transition, that is due to the decrease of the effective control parameter $\alpha^*$. We see the two effects of an increase of the coupling *D*: it promotes the links between sites inducing a disorder-order phase transition and reinforces the influence of the SW sites on the rest of the system, inducing an order-disorder phase transition.

Trajectories in Fig. 7 diverge for finite and positive $\alpha^*$ if

$$\alpha+\Delta(2p_+-1)>0. \tag{19}$$

If this condition is fulfilled, the system presents a single disorder-order transition. On the other hand, if $\alpha+\Delta(2p_+-1)<0$, there can be either no transition at all or a reentrant transition. This condition allows us to reproduce a number of features of the phase diagrams of Figs. 1 and 3. For $\alpha<0$ (Fig. 1), if $p_+<1/2$ we have either DOD or no transition, whereas if $p_+>1/2$ there is DO transition for $\Delta>|\alpha|/(2p_+-1)$. This implies that the curves in Fig. 1 for $p_+>1/2$ have a vertical asymptote at $\Delta=|\alpha|/(2p_+-1)$. For $\alpha>0$ (Fig. 3), if $p_+>1/2$ we have DO transition for any value of $\Delta$, whereas if $p_+<1/2$ there is DO transition only for $\Delta<\alpha/(1-2p_+)$. This also locates at $\Delta=\alpha/(1-2p_+)$ the vertical asymptotes of all the curves in Fig. 3.

The decimation technique also accounts for the phase transitions occurring by increasing $\Delta$. In Fig. 8 we have plotted on the phase diagram of the nonrandom GL model the trajectories resulting from varying $\Delta$ with $\alpha=0.75$, $D=4$ and several values of $p_+$. $D^*$ is a decreasing function of $\Delta$ but $\alpha^*$ does not have a monotonous behavior. In any case, we can clearly see the ODO transitions in the figure. More-

over, Eq. (18) tells us that for $\Delta \to \infty$ we have $D^* = Dp_+$ and $\alpha$ diverges. Therefore, the system is in an ordered phase for $\Delta \to \infty$ for any value of the other parameters (assuming $D \neq 0$).

### B. The random Blume-Capel model

One of the most important results of the present work is the generality of the mechanism behind both the DOD and ODO phase transitions: external fluctuations (impurities) producing the mixture of two dynamics. We expect to find a similar behavior in a number of different systems. To support this idea, here we study the phase diagram of the so-called Blume-Capel (BC) model [25], a spin-1 system with Hamiltonian,

$$\mathcal{H}_{BC}(\{S_i\}) = \sum_{i=1}^{N} \left\{ U(S_i) - J \sum_{\langle ji \rangle} S_j S_i \right\}, \tag{20}$$

where $S_i$ is the spin variable that takes the values $0, \pm 1$.

This model was proposed to describe the critical behavior of $^3$He-$^4$He mixtures. The $^3$He atoms are represented by the state $S=0$, and $^4$He by $S=\pm 1$. The phase transition to a superfluid state corresponds to a symmetry breaking between $S=\pm 1$ states.

The term $U(S_i) = -\lambda S_i^2/2$ is the local potential at each site. Note that $\lambda$ plays the equivalent role of $\alpha$ in the local potential of the GL model. In the BC model if $\lambda < 0$, the local dynamics favors the zero spin solution, whereas if $\lambda > 0$ the nonzero spin solutions are energetically more favorable.

The inclusion of external fluctuations in the local dynamics of the BC model will ensure one of the ingredients needed for the appearance of DOD and ODO phase transitions, dynamics mixture. Consequently, we perturb the BC control parameter $\lambda$ with quenched dichotomous fluctuations with probability density (3) obtaining the following site-dependent local potential,

$$U(S_i;\zeta_i) = -\frac{\lambda + \zeta_i}{2} S_i^2 . \tag{21}$$

This random version of the BC model has been recently proposed in the context of the critical behavior of a mixture of $^3$He and $^4$He in random media, particularly an aerogel [22]. One of the most striking results, when including random fields in such a model, is the elimination of first-order phase transitions.

To clarify the relationship between the random BC and GL models, let us define $D = 4dJ$ and $\alpha = \lambda + D$. In terms of these parameters, the Hamiltonian of the random BC model now reads

$$\mathcal{H}_{RBC}(\{S_i\};\{\zeta_i\}) = \sum_{i=1}^{N} \left\{ -\frac{\alpha + \zeta_i}{2} S_i^2 + \frac{D}{8d} \sum_{\langle ji \rangle} (S_j - S_i)^2 \right\}. \tag{22}$$

The replica symmetry ansatz gives us the following equation for the critical points (see the Appendix):

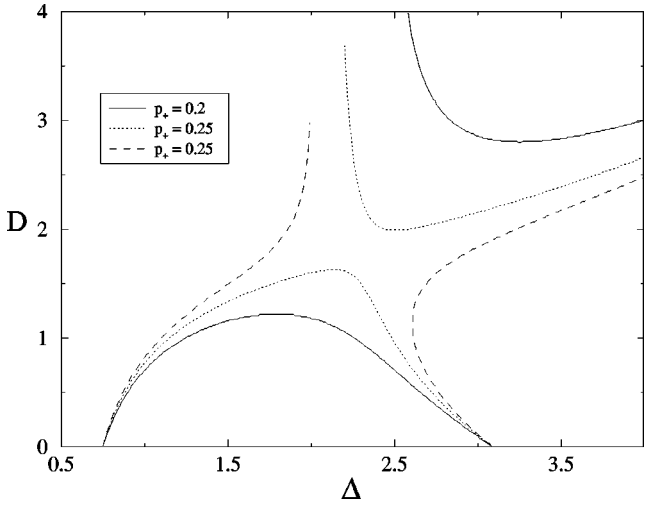


FIG. 9. $(\Delta, D)$ phase diagram for the random Blume-Capel model for different values of $p_+$ ($\beta = 2$, $\alpha = 0.75$). Note the saddle-point structure and the reentrant DOD and ODO phase transitions very similar to those occurring in the random GL model.

$$\frac{1}{D} = \frac{p_+}{1 + \frac{1}{2} e^{D - \alpha - \Delta}} + \frac{p_-}{1 + \frac{1}{2} e^{D - \alpha + \Delta}}, \tag{23}$$

where we have chosen $\beta = 2$ in order to compare with the results for the GL model. In Fig. 9 we plot the phase diagram in the $(\Delta, D)$ plane for different values of $p_+$ and $\alpha = 0.75$. As in the random GL model, the random BC system also shows DOD and ODO reentrant phase transitions and the saddle-point structure as $p_+$ changes.

## VI. CONCLUSIONS AND PERSPECTIVES

In this work we used different analytical techniques and also numerical simulations to show the existence of two counterintuitive reentrant phase transitions in the GL model perturbed by quenched dichotomous fluctuations.

Disorder-order-disorder transitions appear when the coupling increases. The fact that the coupling can destroy an ordered phase was first found in a nonequilibrium phase transition induced by colored noise [19]. Here we have shown that the same phenomenon can be observed in equilibrium disordered system.

We have characterized order-disorder-order transitions when the intensity of the noise increases. This sequence of transitions is the opposite to those found in nonequilibrium models where weak noise has an ordering role whereas strong noise is destructive.

We have also given an intuitive explanation of these reentrant phase transitions using a decimation technique that allows to map trajectories in the phase diagram of the random system into trajectories in a nonrandom GL model.

Our work may be relevant to different situations regarding anisotropic ferromagnets. The model considered can describe the critical behavior of a conglomerate made by two kinds of anisotropic ferromagnets with different critical temperatures. In this context, a simple experiment could be devised to check some of the results obtained in this work, as the mag-

netization of a *single* anisotropic ferromagnet could be driven through ODO reentrant phase transitions by heating the material in a random arrary of points in a dichotomous way.

Moreover, as already mentioned in the Introduction, the GL model is a fundamental model that appears in many problems of critical phenomena. We have studied the influence of dichotomic disorder for a conserved model, the model *A*, but we expect this type of disorder to be relevant to other kinds of dynamics as phase separation (model *B*), structural transitions (model *C*), binary fluids (model *H*), or superfluid phases (model *F*).

Most of the features discussed for the random GL model are also exhibited by a random Blume-Capel model, used to describe the critical behavior of helium mixtures in a random media, showing that our results do not depend on the details of the model and are present whenever a system possesses two types of local dynamics with one and two stable states.

Finally, we want to briefly discuss the guidelines for future work on the field. The inclusion of a finite correlation-time perturbation on the external fluctuations will induce non-equilibrium noise-induced phase transitions. In particular, the results of Refs. [12,13] should be recovered when the correlation time vanishes. Therefore, finite correlation time should provide information about the crossover between these two models. We then expect an even richer phenomenology and, in particular, the appearance of a characteristic correlation time for which the reentrant character of the transitions vanishes. Work in this direction is in progress.

## ACKNOWLEDGMENTS

We are indebted to David Mukamel, Elka Korutcheva, and Mariano Revenga for fruitful comments and discussions during the elaboration of this work. This work has been financially supported by the DGES (Spain) Project No. PB97-0076 and by the ISI Foundation (EU HC&M Network ERBCHRX-CT940546).

## APPENDIX QUENCHED AND ANNEALED IMPURITIES

The macroscopic properties of disordered systems in equilibrium can be calculated by means of two types of averages over the configurations of disorder: quenching and annealing. The former corresponds to quenched or frozen impurities and the latter to impurities that evolve and thermalize at the time scale of measurement.

The starting point of both averages is the partition function of the system for a given disorder configuration:

$$\mathcal{Z}=\int_{\mathbb{R}^N} d\vec{\psi}\,\exp[-\beta\mathcal{H}(\{\psi_i\},\{\zeta_i\})], \tag{A1}$$

where $d\vec{\psi}=\Pi_{i=1}^{N} d\psi_i$ and $\mathcal{H}(\{\psi_i\},\{\zeta_i\})$ is the globally coupled Hamiltonian (14) of the system that depends on the field $\{\psi_i\}$ and also on the disorder $\{\zeta_i\}$. This makes the model simpler than systems where disorder affects the coupling between sites, as the Sherrington-Kirkpatrick model [26].

Using the Hubbard-Stratonovich transformation:

$$e^{ay^2}=\frac{1}{\sqrt{2\pi}}\int_{\mathbb{R}}\exp(-x^2/2+xy\sqrt{2a})\,dx, \tag{A2}$$

with $y=\Sigma_i\psi_i$ and $a=\beta D/(2N)$, and defining $m\equiv x\sqrt{\beta/(4DN)}$, the partition function can be written as

$$\mathcal{Z}=\sqrt{\frac{2DN}{\beta\pi}}\int_{\mathbb{R}} dm\int_{\mathbb{R}^N} d\vec{\psi}\exp\left[-\beta\sum_{i=1}^{N}\left(V(\psi_i;\zeta_i)+\frac{D}{2}\psi_i^2\right)-\frac{2DN}{\beta}m^2+2Dm\sum_{i=1}^{N}\psi_i\right]. \tag{A3}$$

After some simple manipulations, Eq. (A3) becomes

$$\mathcal{Z}=\int_{\mathbb{R}} dm\int_{\mathbb{R}^N} d\vec{\psi}\prod_{i=1}^{N} \mathrm{e}^{f(\psi_i;m)}, \tag{A4}$$

where

$$f(\psi_i;m)=-\beta\left(V(\psi_i,\zeta_i)+\frac{D}{2}\psi_i^2\right)-\frac{2D}{\beta}m^2+2Dm\psi_i+\frac{1}{2N}\ln\left(\frac{2DN}{\beta\pi}\right). \tag{A5}$$

Annealing averages are derived from the annealing free energy $\mathcal{F}_{\mathrm{ann}}=-\ln\langle\mathcal{Z}\rangle/\beta$ where $\langle\cdot\rangle$ denotes the average over configurations of disorder. Averaging Eq. (A4) gives

$$\begin{aligned}\langle\mathcal{Z}\rangle&=\int_{\mathbb{R}} dm\left\langle\int_{\mathbb{R}^N} d\vec{\psi}\prod_{i=1}^{N}\mathrm{e}^{[f(\psi_i;m)]}\right\rangle\\&=\int_{\mathbb{R}} dm\left\langle\int_{\mathbb{R}} d\psi\,\mathrm{e}^{[f(\psi;m)]}\right\rangle^{N}\\&=\int_{\mathbb{R}} dm\;\mathrm{e}^{[NF(m)]},\end{aligned} \tag{A6}$$

where we have used the fact that $\zeta_i$ are independent random variables. The function $F(m)$ is given by

$$F(m)\equiv\frac{1}{2N}\ln\left(\frac{2DN}{\beta\pi}\right)-\frac{2D}{\beta}m^2+\ln\int_{\mathbb{R}} d\psi\langle\exp[-\beta V(\psi;\zeta)]\rangle\times\exp[-(\beta D/2)\psi^2+2Dm\psi]. \tag{A7}$$

In the thermodynamic limit, $N\to\infty$, only the saddle points of $F(m)$ contribute to the integral in Eq. (A6). The saddle points are the solutions of the equation $F'(m)=0$, i.e.,

$$m=\frac{\beta}{2}\int_{\mathbb{R}} d\psi\;\;\psi\;\;P_{\mathrm{ann}}(\psi;m) \tag{A8}$$

where $P_{\mathrm{ann}}(\psi;m)$ is the probability distribution,

$$P_{\rm ann}(\psi;m)=N(m)\langle\exp[-\beta V(\psi;\zeta)]\rangle \times\exp\left(-\frac{\beta D}{2}\psi^2+2Dm\psi\right) \tag{A9}$$

$N(m)$ being a normalization constant. If $\zeta_i$ are dichotomous variables, as in the model studied in the paper, we have

$$P_{\rm ann}(\psi;m)=N(m)[p_+\exp\{-\beta V(\psi;\Delta)\} +p_-\exp\{-\beta V(\psi;-\Delta)\}] \times\exp\left(-\frac{\beta D}{2}\psi^2+2Dm\psi\right). \tag{A10}$$

The solution $m$ of Eq. (A8) is the annealing average of $\Sigma_{i=1}^N\psi_i/N$ in the thermodynamic limit. Then, the phase diagram of the system can be found by a similar analysis as the one carried out in Sec. II. Equation (A8) plays identical role as the self-consistency equation (11) and so does $m$ as $\langle\psi\rangle$. Notice, however, that $P_{\rm ann}(\psi;m)$ is not equal to $P_{\rm st}(\psi;\langle\psi\rangle)$ in Eq. (9), which leads to different phase diagrams from those calculated in Sec. II.

On the other hand, quenched averages are obtained from the quenching free energy $\mathcal{F}_{\rm quen}=-(1/\beta)\langle\ln\mathcal{Z}\rangle$. The average of the logarithm can be calculated using the replica trick [26]:

$$\langle\ln\mathcal{Z}\rangle=\lim_{n\to0}\frac{\langle\mathcal{Z}^n\rangle-1}{n}. \tag{A11}$$

The average $\langle\mathcal{Z}^n\rangle$ can be interpreted as the partition function of a set of $n$ replicas of the system. The replicas do not interact with each other but the configuration of disorder is the same for all of them. Consequently, they are not statistically independent. The average of $\mathcal{Z}^n$ can be written as

$$\langle\mathcal{Z}^n\rangle=\int_{\mathbb{R}^n}\left(\prod_{\gamma=1}^n dm_\gamma\right)\left\langle\prod_{\gamma=1}^n\int_{\mathbb{R}}d\psi_\gamma\exp[f(\psi_\gamma;m_\gamma)]\right\rangle^N =\int_{\mathbb{R}^n}\left(\prod_{\gamma=1}^n dm_\gamma\right)\exp[N\tilde{F}(\{m_\gamma\})], \tag{A12}$$

with

$$\tilde{F}(\{m_\gamma\})=\frac{n}{2N}\ln\left(\frac{2DN}{\beta\pi}\right)-\frac{2D}{\beta}\sum_{\gamma=1}^n m_\gamma^2 +\ln\left\langle\prod_{\gamma=1}^n\int_{\mathbb{R}}d\psi_\gamma\exp[-\beta V(\psi_\gamma;\zeta)] \times\exp\left(-\frac{\beta D}{2}\psi_\gamma^2+2Dm_\gamma\psi_\gamma\right)\right\rangle. \tag{A13}$$

Once more, the integral in Eq. (A12) could be solved in the thermodynamic limit by finding the saddle points of $\tilde{F}(\{m_\gamma\})$. In this case, further assumptions have to be made. First, the *replica symmetry ansatz*, which assumes that the relevant saddle points are those with $m_\gamma=m$ for all $\gamma$. With this, the function $\tilde{F}$ on this subspace reads:

$$\tilde{F}(m)=\frac{n}{2N}\ln\left(\frac{2DN}{\beta\pi}\right)-\frac{2Dn}{\beta}m^2+\ln\left\langle\left[\int_{\mathbb{R}}d\psi \times\exp\{-\beta V(\psi;\zeta)\}\exp\left(-\frac{\beta D}{2}\psi^2+2Dm\psi\right)\right]^n\right\rangle. \tag{A14}$$

Second, we assume that the limits $n\to0$ and $N\to\infty$ commute and the function $\tilde{F}(m)$ can be analytically extended for noninteger $n$ and expanded around $n=0$ as

$$\begin{aligned}\tilde{F}(m)&\simeq\frac{n}{2N}\ln\left(\frac{2DN}{\beta\pi}\right)-\frac{2Dn}{\beta}m^2+\ln\left\langle 1+n\ln\int_{\mathbb{R}}d\psi \times\exp[-\beta V(\psi;\zeta)]\exp\left(-\frac{\beta D}{2}\psi^2+2Dm\psi\right)\right\rangle\\ &\simeq n\left[\frac{1}{2N}\ln\left(\frac{2DN}{\beta\pi}\right)-\frac{2D}{\beta}m^2+\left\langle\ln\int_{\mathbb{R}}d\psi \times\exp[-\beta V(\psi;\zeta)]\exp\left(-\frac{\beta D}{2}\psi^2+2Dm\psi\right)\right\rangle\right].\end{aligned} \tag{A15}$$

Thus, the equation for the saddle points of $\tilde{F}(m)$ is

$$m=\frac{\beta}{2}\int_{\mathbb{R}}d\psi\ \ \psi\ \ P_{\rm quen}(\psi;m), \tag{A16}$$

where $P_{\rm quen}(\psi;m)$ is the probability distribution

$$P_{\rm quen}(\psi;m)=\left\langle\frac{\exp\left[-\beta V(\psi;\zeta)-\frac{\beta D}{2}\psi^2+2Dm\psi\right]}{\int_{\mathbb{R}}d\psi\exp\left[-\beta V(\psi;\zeta)-\frac{\beta D}{2}\psi^2+2Dm\psi\right]}\right\rangle. \tag{A17}$$

If $\zeta_i$ are dichotomous variables we recover the self-consistency equation (11) and thus the same phase diagram. Therefore, we have proven that the mean-field analysis of Sec. II is equivalent to quenching averages under the assumption of symmetry of replicas.

Quenching and annealing give rather different phase diagrams. As mentioned in Sec. VI, we expect that the GL model perturbed by dichotomous noise with finite correlation time will give a phase diagram similar to the one obtained by using annealing averages.

[1] S-K. Ma, *Modern Theory of Critical Phenomena* (Benjamin-Cummings, Reading, 1976).
[2] M. E. Fisher, Rev. Mod. Phys. **46**, 597 (1974); **79**, 653 (1998), and references therein.
[3] T. C. Lubensky, Phys. Rev. B **11**, 3573 (1975).
[4] P. C. Hohenberg and B. I. Halperin, Rev. Mod. Phys. **49**, 435 (1977).
[5] R. Toral and A. Chakrabarti, Phys. Rev. B **42**, 2445 (1990).
[6] D. I. Uzunov, *Theory of Critical Phenomena* (World Scientific, Singapore, 1993), and references therein.
[7] O. T. Valls and G. F. Mazenko, Phys. Rev. B **34**, 7941 (1986).
[8] A. I. Larkin, Zh. Éksp. Teor. Fiz. **58**, 1466 (1970) [ Sov. Phys. JETP **31**, 784 (1970)].
[9] A. I. Larkin and Y. N. Ovchinnikov, Zh. Éksp. Teor. Fiz. **61**, 1271 (1972) [ Sov. Phys. JETP **34**, 651 (1972)].
[10] V. Dotsenko, A. B. Harris, D. Sherrington, and R. B. Stinchcombe, J. Phys. A **28**, 3093 (1995); V. S. Dotsenko, *ibid.* **32**, 2949 (1999).
[11] E. Korutcheva and F. J. de la Rubia, Phys. Rev. B **58**, 5153 (1998).
[12] C. Van den Broeck, J. M. R. Parrondo, J. Armero, and A. Hernández-Machado, Phys. Rev. E **49**, 2639 (1994).
[13] J. García-Ojalvo, J. M. R. Parrondo, J. M. Sancho, and C. Van den Broeck, Phys. Rev. E **54**, 6918 (1996).
[14] J. García-Ojalvo and J. M. Sancho, *Noise in Spatially Extended Systems* (Springer, New York, 1999).
[15] C. Van den Broeck, J. M. R. Parrondo, and R. Toral, Phys. Rev. Lett. **73**, 3395 (1994); C. Van den Broeck, J. M. R. Parrondo, R. Toral, and R. Kawai, Phys. Rev. E **55**, 4084 (1997).
[16] J. M. R. Parrondo, C. Van den Broeck, J. Buceta, and F. J. de la Rubia, Physica A **224**, 153 (1996).
[17] R. Müller, K. Lippert, A. Kühnel, and U. Behn, Phys. Rev. E **56**, 2658 (1997).
[18] W. Genovese, M. A. Muñoz, and J. M. Sancho, Phys. Rev. E **57**, R2495 (1998).
[19] S. Mangioni, R. Deza, H. S. Wio, and R. Toral, Phys. Rev. Lett. **79**, 2389 (1997).
[20] S. Kim, S. H. Park, and C. S. Ryu, Phys. Rev. E **58**, 7994 (1998).
[21] J. García-Ojalvo and J. M. Sancho, Phys. Rev. E **49**, 2769 (1994).
[22] A. Maritan, M. Cieplak, M. R. Swift, F. Toigo, and J. R. Banavar, Phys. Rev. Lett. **69**, 221 (1992); C. Buzano, A. Maritan, and A. Pelizzola, J. Phys.: Condens. Matter **6**, 327 (1994); N. S. Branco and B. M. Boechat, Phys. Rev. B **56**, 11 673 (1997).
[23] A. D. Bruce, Adv. Phys. **29**, 111 (1980).
[24] K. Binder and D. W. Heermann, *Montecarlo Simulations in Statistical Physics* (Springer-Verlag, Berlin, 1988).
[25] M. Blume, Phys. Rev. **141**, 517 (1966); H. W. Capel, Physica (Amsterdam) **32**, 966 (1966).
[26] D. Sherrington and S. Kirkpatrick, Phys. Rev. Lett. **35**, 1792 (1975).